BRAIN COMMUNICATIONS

Dynamic connectivity predicts acute motor impairment and recovery post-stroke

Anna K. Bonkhoff,[1,2] Anne K. Rehme,[3] Lukas Hensel,[3] Caroline Tscherpel,[2,3] Lukas J. Volz,[3] Flor A. Espinoza,[5] Harshvardhan Gazula,[4,5] Victor M. Vergara,[5] Gereon R. Fink,[2,3] Vince D. Calhoun,[5] Natalia S. Rost[1] and Christian Grefkes[2,3]

Thorough assessment of cerebral dysfunction after acute lesions is paramount to optimize predicting clinical outcomes. We here built random forest classifier-based prediction models of acute motor impairment and recovery post-stroke. Predictions relied on structural and resting-state fMRI data from 54 stroke patients scanned within the first days of symptom onset. Functional connectivity was estimated via static and dynamic approaches. Motor performance was phenotyped in the acute phase and 6 months later. A model based on the time spent in specific dynamic connectivity configurations achieved the best discrimination between patients with and without motor impairments (out-of-sample area under the curve, 95% confidence interval: 0.67 ± 0.01). In contrast, patients with moderate-to-severe impairments could be differentiated from patients with mild deficits using a model based on the variability of dynamic connectivity (0.83 ± 0.01). Here, the variability of the connectivity between ipsilesional sensorimotor cortex and putamen discriminated the most between patients. Finally, motor recovery was best predicted by the time spent in specific connectivity configurations (0.89 ± 0.01) in combination with the initial impairment. Here, better recovery was linked to a shorter time spent in a functionally integrated configuration. Dynamic connectivity-derived parameters constitute potent predictors of acute impairment and recovery, which, in the future, might inform personalized therapy regimens to promote stroke recovery.

1 J. Philip Kistler Stroke Research Center, Department of Neurology, Massachusetts General Hospital, Boston, MA 02114, USA
2 Cognitive Neuroscience, Institute of Neuroscience and Medicine (INM-3), Research Centre Juelich, 52425 Juelich, Germany
3 Medical Faculty, University of Cologne, and Department of Neurology, University Hospital Cologne, 50937 Cologne, Germany
4 Princeton Neuroscience Institute, Princeton University, Princeton, NJ 08540, USA
5 Tri-institutional Center for Translational Research in Neuroimaging and Data Science (TReNDS), Georgia State University, Georgia Institute of Technology, Emory University, Atlanta, GA 30303, USA

Correspondence to: Christian Grefkes, MD PhD
Department of Neurology, University Hospital Cologne, Kerpener Str. 62, 50937 Cologne, Germany
E-mail: christian.grefkes@uk-koeln.de

Keywords: ischemic stroke; upper limb motor impairment; recovery post-stroke; dynamic functional network connectivity; precision medicine

Abbreviations: AUC = area under the curve, dFNC = dynamic functional network connectivity, FDR = false discovery rate, MI-UL = Motricity Index of the upper limb, rsfMRI = resting-state functional magnetic resonance imaging

Received February 12, 2021. Revised May 29, 2021. Accepted August 12, 2021. Advance Access publication September 30, 2021

Graphical Abstract

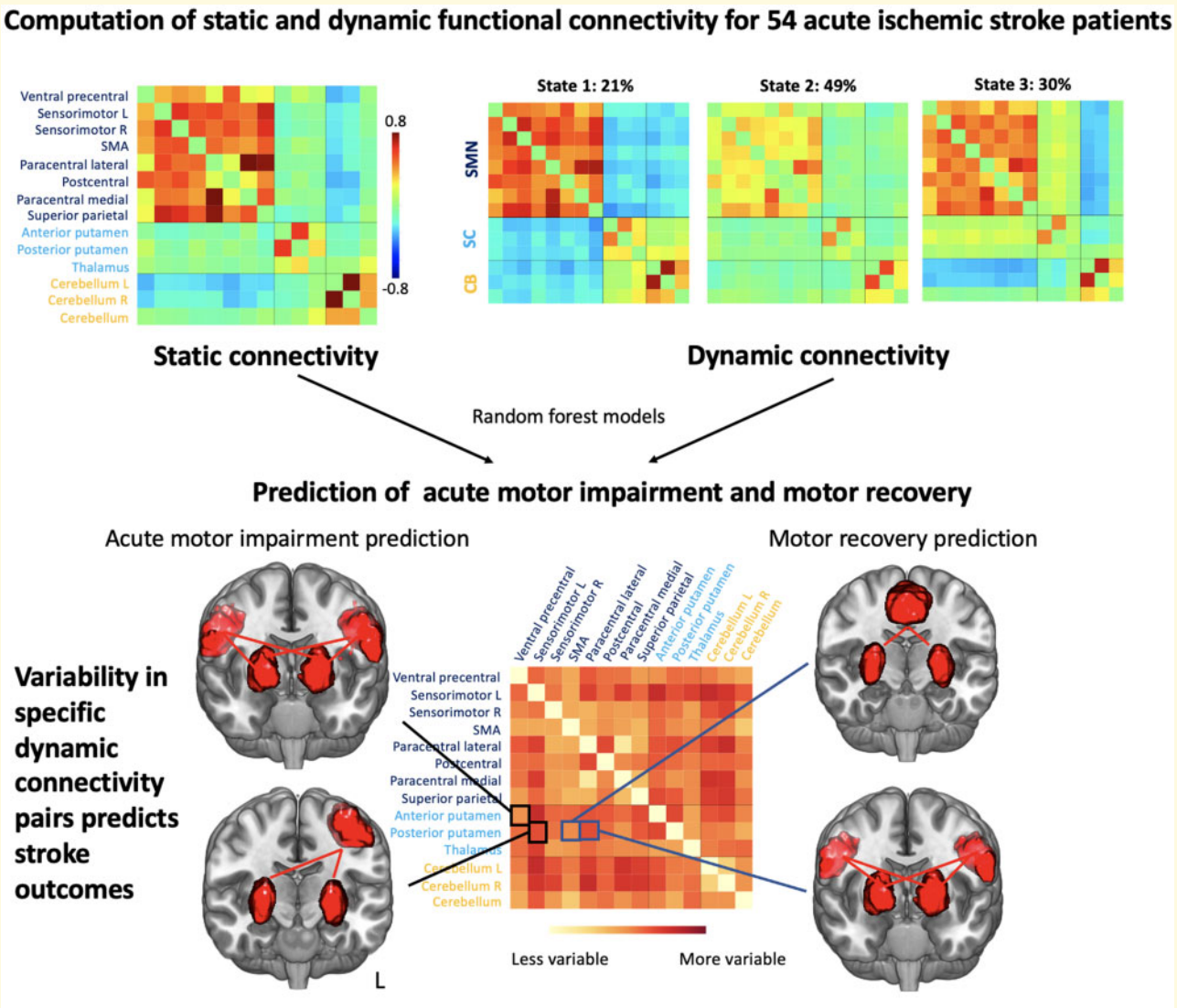

Introduction

Stroke is the leading cause of long-term disability in adults[1] and entails the highest number of disability-adjusted life years among more than 300 different diseases.[2] To optimize stroke care, it is of great importance to establish prediction models of stroke-related disabilities at the single patient level. These predictions may not only inform patients and their proxies about individual trajectories after stroke, but may also facilitate the allocation and planning of targeted rehabilitative regimens.

The amount of initial motor impairment has been frequently demonstrated to constitute a strong predictor of chronic impairment,[3] yet may not guarantee sufficiently accurate predictions at the level of single patients.[4] This limitation motivates the consideration of further biomarkers of stroke recovery.[5] While structural and functional neuroimaging-derived information have proven viable candidates, only a few studies have been published aiming at predicting motor recovery as a long-term outcome.[6–8] Novel techniques permit the increase in the temporal resolution of MRI resting-state functional connectivity maps from minutes to seconds, thereby offering a new vista on the neural mechanisms driving functional recovery[9–11] We have recently shown that dynamic functional network connectivity (dFNC) analyses provide new information on cerebral alterations post-stroke, thus far hidden in conventional resting-state analyses that assume static connectivity between brain regions.[12] Several studies suggest that dFNC may not only enhance inferences in imaging correlates of brain disease, but also lead to substantial increases in predictive capacities for several

of these diseases, potentially as the dynamic approach may to be closer to the neurobiology underlying brain function.[13–15]

Therefore, we here sought to explore the potential of dFNC parameters for predicting acute motor impairment and recovery after stroke, as well as for granting further insights into pathophysiological cerebral mechanisms post-stroke. We hypothesized that dFNC parameters obtained in the acute post-stroke phase are superior to static connectivity for predicting motor outcome, as neural reorganization enabling recovery of function might especially depend on the dynamic flexibility of neural network.[12] Furthermore, we expected enhanced prediction performances for dFNC-informed models compared to those that solely employed clinical predictors, such as an initial impairment score, or structural lesion information.

Methods

Participants

Fifty-four patients admitted to the University Hospital of Cologne, Department of Neurology, due to acute first-ever ischaemic stroke participated in this study (c.f., Supplementary materials for inclusion criteria, first assessment on average three days after stroke onset). For $n = 30$ patients, follow-up visits could be scheduled on average 30 weeks after the ischaemic event. Patients received rehabilitation measures, e.g. physiotherapy and occupational therapy, according to general standards in Germany. All patients received some form of physical and/or occupational therapy for at least three weeks. Patients with persistent deficits usuallycontinue to receive one to two 30-minutes sessions of out-patient rehabilitation therapy per week. The study was approved by the local ethics committee, and all patients provided informed written consent following the Declaration of Helsinki.

Motor performance and recovery

Upper limb motor performance was tested twice: at the time of scanning ($n = 54$), i.e. in the acute post-stroke phase and at follow-up six months later. Individual motor performance was captured via the Motricity Index of the affected upper limb (MI-UL,[16] c.f., Supplementary Table 1). Patients were categorized in three subgroups depending on the level of motor impairment: (i) patients with no upper limb impairment (MI-UL = 33, $n = 26$); (ii) patients with mild impairments ($25 \leq$ MI-UL ≤ 32, $n = 16$); and (iii) patients with moderate-to-severe upper limb motor impairment (MI-UL ≤ 22, $n = 12$). The cut-off between mildly and moderate-to-severely affected patients was chosen based on the sample distribution of MI-UL scores of patients with impairments and a median score of MI-UL = 25.3. As a consequence, patients in the moderate-to-severe group featured an MI-UL of maximal 22. Given that three movements were tested, i.e. shoulder abduction, elbow flexion and pinch grip, MI-UL scores below or equal to 22 could arise from varying combinations of motor impairments, e.g. the inability for all three movements of performing them against gravity or more severe limitations of one movement, e.g. no hand movement, but visible movements for shoulder abduction and elbow flexion. In any case, at least one of the tested movements could necessarily not be performed against resistance, which may be seen equivalent to a clinically relevant motor deficit.

Recovery was quantified as change between follow-up and acute motor impairment ($\text{MI-UL}_{\text{Follow-up}}$—$\text{MI-UL}_{\text{acute}}$). In particular, we defined three subgroups which differed in the amount of experienced motor recovery: (i) no change in motor function ($n = 16$, no change could be due to no initial impairment or no change between initial and follow-up impairment); (ii) more ($n = 9$); and (iii) less pronounced recovery ($n = 5$). The cut-off between more and less pronounced recovery was based on the median amount of recovery in the sample of all patients with an initial impairment (recovery = 7.7 MI points). The difference between the two adjacent MI categories, i.e. 'palpable contraction, but no movement' versus 'visible movement, but full range and not against gravity' or 'Full movement against gravity, but weaker than on the other side' and 'Normal power', is on average 6.6 points. Our cut-off value of 7.7 hence represents a noticeable and relevant amount of recovery.

MRI acquisition

Resting-state fMRI data were acquired in the framework of a clinical imaging protocol in a clinical routine on a 1.5 T scanner (Philips, Guildford, UK). Patients were asked to lie motionless in the scanner and stay awake. Gradient echo-planar imaging (EPI) parameters were as follows: repetition time (TR)=2100 ms, echo time (TE)=50 ms, field of view (FOV)=250 mm, 24 axial slices, voxel size: $3.9 \times 3.9 \times 3.9$ mm^3, 183 volumes, acquisition time: ~six minutes. We, furthermore, obtained the following structural scans: diffusion-weighted imaging (DWI) images (TR = 3900 ms, TE = 95 ms, FOV = 230 mm, 22 axial slices, voxel size = $1.8 \times 3 \times 6$ mm^3) and T_2-weighted MR-images (TR = 5600 ms, TE = 110 ms, FOV = 230 mm, 22 axial slices, voxel size = $0.9 \times 1.1 \times 6.0$ mm^3) for more detailed analyses of lesion topography. Images of patients with right-hemispheric lesions ($n = 19$) were flipped at the midsagittal plane.[8,17] As a consequence, no conclusions on hemispheric-specific effects can be drawn with respect to motor recovery.

Structural MRI analysis

Stroke lesion maps were constructed by manually segmenting lesioned tissue on DWI images using MRIcron.[18] Subsequently, DWI images, as well as corresponding

lesion masks, were normalized to standard MNI-space by first co-registering images to an MNI-template and then employing the unified segmentation algorithm after masking infarcted tissue.[19] Lesion maps of 53 patients passed quality control (in one subject top slices were missing due to an alignment error during DWI volume acquisition). In a subsequent step, we applied principal component analysis (PCA) to reduce the high-dimensional lesioned voxel-space (9900 voxels lesioned in at least one subject). We performed this PCA-step twice and retained (i) all components that individually explained more than 5% of the variance in the first case (*5-component structural lesion data*, 5 components, 64% explained variance in total), and (ii) all components that explained more than 95% of the variance in total in the second case (*28-component structural lesion data*, 28 components).[7]

Resting-state fMRI analysis: pre-processing

Resting-state fMRI data were pre-processed employing Statistical Parametric Mapping (SPM8; http://www.fil.ion.ucl.ac.uk/spm/) in a Matlab framework (The Mathworks 2012a, Natick, MA, USA). As for one subject, only 182 images were acquired, we shortened all further time courses by one volume to harmonize the scan length across subjects. The first three volumes of each time-series were discarded to allow for blood-oxygenation level dependent (BOLD)-signal saturation.

The 179 remaining images were spatially realigned to the time-series' mean image and co-registered with the structural image and corresponding lesion mask. Subsequently, all images were spatially normalized to standard MNI-space using the unified segmentation option after masking lesioned brain tissue. In a final step, data were smoothed by a Gaussian kernel with a full-width at half maximum of 8 mm. For each patient's time series, maximum framewise translation and framewise rotation did not exceed 3 mm and 0.05 rad, respectively, similar to previous work.[12] Moreover, individual motion parameters were integrated as covariates in later analyses.

Intrinsic connectivity networks

To define spatially separated intrinsic connectivity networks, components were extracted employing independent component analysis (ICA)[20,21] on the resting-state functional magnetic resonance imaging (rsfMRI) data of 405 healthy controls (components available for download: http://trendscenter.org/software/).[9,10] Details on the applied group information guided ICA ('back-reconstruction') algorithm can be found in Salman et al.[22]

Because of our focus on motor impairments, we centred the analysis on 14 motor network components that can be grouped into three functional domains: Eight cortical sensorimotor components, three subcortical components and three cerebellar components. Ancillary pre-processing steps comprised time-course de-trending (i.e. accounting for linear, quadratic, and cubic trends in the data), de-spiking using 3Ddespike and application of a fifth-order Butterworth low-pass filter with a high-frequency cut-off of 0.15 Hz. Finally, time-courses were variance normalized.[23]

Static functional network connectivity

For each subject, we computed 'classic' static functional connectivity maps as Fisher's Z-transformed Pearson's pairwise correlation of time-courses between all 14 motor networks, resulting in 91 connectivity pairs. Age, sex, mean framewise translation and rotation were used as independent regressors to correct for demographics and within scanner movement.

Dynamic functional network connectivity

Subsequently, we estimated dFNC within the framework of the sliding window approach.[9,10,24,25] As prior studies suggest that sliding window lengths between 30 and 60 s allow for a successful dFNC estimation with an optimal signal-to-noise ratio,[26] we opted for a window length of 42 s (20 TRs). This step resulted in 159 individual windows that were additionally convolved with a Gaussian of 6.3 s ($\sigma = 3$ TRs). The actual dFNC pairs were obtained from the l_1-regularized precision matrix.[27] The covariates age, sex, mean framewise translation and rotation served as regressors-of-no-interest. Finally, dFNC values were normalized by Fisher's Z-transformation. In the next step, we estimated *connectivity states*, i.e. re-occurring patterns of functional connectivity across time and subject space via k-means clustering of all patients' 159 dFNC matrices.[9,10,28] We relied on the l_1-distance function given its suitability for high-dimensional data.[29] In line with previous work,[9,30] we conducted these clustering processes twice: In the first run, we decided upon the optimal number of clusters k (referred to as states). This optimal number k was determined based on the elbow criterion, which considers the cluster validity index, computed as the ratio between the within-cluster distance to the between-cluster distance.[9] In a second clustering run, each of the 159 windows of all 54 patients was assigned to one of k connectivity states. By these means, we obtained the following dFNC parameters: *fraction times* (the percentage of total time a subject spent in a given connectivity state), *dwell times* (the time a subject spent in a state at any one time without switching to another one) and *number of transitions* (how often a subject changed between states). Furthermore, we computed the variability of actual dFNC pairs by estimating the standard deviation of pairwise functional connectivity over the 159 windows for each patient.[15] The larger this value,

the more the dynamic connectivity varies over the entire duration of the scan.

Statistical analyses I: Group differences in dynamic connectivity variability

To further elucidate the nature of the variability in dFNC strength concerning motor impairments, we evaluated differences in the variability of each dynamic connectivity pair between stroke patients with (i) no motor impairment; (ii) mild motor impairment; and (iii) and moderate-to-severe motor impairment using a three-level one-way ANOVA (level of significance: $P < 0.05$). In case of significant group differences, *post hoc t*-tests were conducted [level of significance: $P < 0.05$, false discovery rate (FDR)-corrected for multiple comparisons]. Furthermore, we repeated these analyses steps of three-level one-way ANOVA and *post hoc t*-tests for the patient sample with follow-up scores. In addition, we performed correlation analyses between the overall variability in dFNC strength (i.e. the average of variability for all dynamic connectivity pairs) and lesion volume, as well as change in motor performance (Spearman correlations, level of significance: $P < 0.05$).

Statistical analyses II: Prediction of acute motor impairment and motor recovery

The main aim of the present study was to build robust prediction models of acute individual motor impairment and recovery within the first months post-stroke based on neuroimaging data acquired in the acute post-stroke phase.

We created two classification scenarios: We aimed at (i) predicting the acute motor deficits from fMRI data acquired in the acute post-stroke phase and (ii) predicting motor recovery. With respect to the first scenario, we initially sought to determine whether it is possible to predict whether a stroke patient has or doesn't have a motor deficit using the MI-UL score. In addition, we tested whether it is also possible to predict the severity of motor impairment, i.e. whether an individual patient had a mild versus a moderate-to-severe impairment of the upper limb. Given that acute impairment itself can, in principle, be determined via clinical assessment in a few minutes without the necessity to employ any prediction algorithm, the main focus of these initial analyses was to extract predictive features with potential pathophysiological meaning, facilitating a greater neuroscientific insight. With respect to the second prediction scenario, we aimed to predict motor recovery, i.e., the change between the follow-up six months post-stroke and the acute MI-UL-score. As we considered three categories of motor recovery (no motor recovery, minor recovery, substantial recovery), we extended previous two-class prediction scenarios to a multi-class prediction one. In an exploratory analysis, we also computed a prediction model to differentiate between patients with minor to no recovery ($n = 8$) and patients with substantial recovery ($n = 9$).

A random forest classifier was used as prediction model.[31] This meta-estimator machine learning algorithm fits several decision tree classifiers on bootstrapped subsamples of the dataset and successively averages individual predictions. In this way, it aims to increase prediction accuracy by reducing variance and overfitting. Moreover, random forest classifiers can automatically include non-linear and interaction effects of input variables and handle correlated input variables favourably.[32] Given our moderate sample size, we accepted the possibility of slightly lower prediction performances, yet avoided an additional nested cross-validation step by adopting hyperparameter settings that were suggested by Olson et al.[33] (n_estimators = 500; criterion = 'entropy', max_features = 0.25). Olson et al. had extracted these settings as the most advantageous ones after running hyperparameter optimizations in 165 biomedical

Table 1 Demographics, clinical and MRI characteristics of all 54 stroke patients (mean and standard deviation, if not indicated otherwise)

	Acute phase ($n = 54$)	Follow-up phase ($n = 30$)
Age	71.9 ± 11.8 years	73.3 ± 10.4 years
Sex (females)	46 %	47 %
Mean Framewise Translation	0.22 ± 0.13 mm	0.24 ± 0.12 mm
Mean Framewise Rotation	0.002 ± 0.001 rad	0.002 ± 0.001 rad
Time since stroke	2.5 ± 1.5 days	210 ± 57 days
Acute: modified Rankin Scale (median, interquartile range, only patients with an initial deficit)	2.0 (2.0) ($n = 24$)	1.0 (1.5) ($n = 15$)
Acute: MI UL *affected arm* (median, interquartile range, only patients with an initial deficit)	25.33 (6.67) ($n = 28$)	25.33 (4.33) ($n = 17$)
Follow-up: MI UL *affected arm* (median, interquartile range, only patients with an initial deficit)	–	33.0 (7) ($n = 17$)
Normalized lesion volume (median, interquartile range)	2240 mm^3 (4768)	4048 mm^3 (10 020)

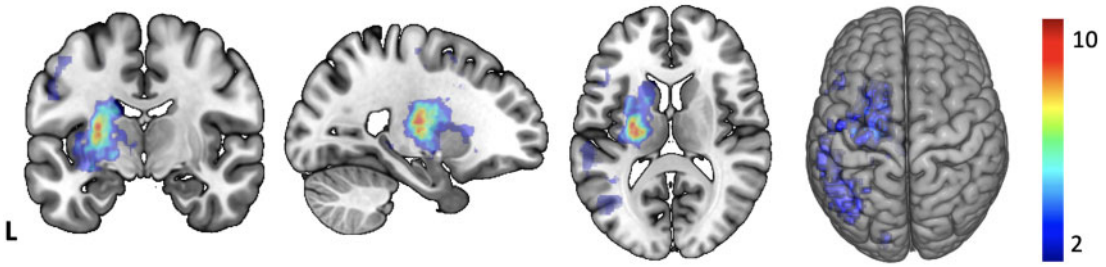

Figure 1 Lesion overlap of all patients. Most lesions were located in the middle cerebral artery territory. The highest lesion load was found subcortically, affecting white matter pathways and the grey matter of basal ganglia. Of note, our sample included five patients with pontine brainstem infarcts and one patient with small bilateral cerebellar lesions in addition to a primary left-hemispheric subcortical stroke. Right-hemispheric lesions of 19 patients were flipped to the left hemisphere to decrease the spatial heterogeneity of lesions.

datasets. To obtain a performance estimate for unseen patient data, i.e. the model's generalization capacity, we conducted 100 randomly initiated 5-fold cross-validations, repeatedly training and testing models in 100×5 training and test sets. In the multi-class recovery prediction analyses, we employed 3-fold cross-validation given the small subgroup sample size.

The reported main performance measure denotes the out-of-sample area under the curve (AUC) and the respective 95% confidence interval, as estimated in 100 randomly initiated 5-fold cross-validations. AUC values range between 0 and 1, and values greater than an AUC = 0.5 are considered to be above chance level. Non-overlapping 95% confidence intervals between models determined significant differences between AUC outcomes. Sensitivity and specificity are given in the Supplementary materials. We also examined the feature importance estimated by the random forest classifier to increase the interpretability of the prediction approach and extract the potential neurophysiological meaning of input features.

Concerning input features, we examined the predictive capacity of neuroimaging features derived from (i) *structural* data; (ii) *static*; and (iii) *dynamic* functional connectivity data. Structural lesion information was considered either in the 5- or 28-component PCA-reduced form. Static functional connectivity was entered as 91 network-pair-wise connectivity values. Finally, we constructed two models relying on dFNC. The first dFNC model was based on the dynamic parameters fraction and dwell times, as well as the number of transitions. The second dFNC model leveraged the variability in the dynamic connectivity of all 91 network pairs. Models were built with and without the addition of the acute motricity index when predicting the recovery after stroke.

Data and code availability

DFNC was computed based on Matlab2019a scripts available in the GIFT toolbox. Further statistical analyses were conducted in a jupyter notebook environment (Python 3.7).

Results

Fifty-four patients participated in this study [mean age: 71.9 (11.8) years, 46% female, days post-stroke: 2.5 (1.5), Table 1]. The majority of their lesions were located subcortically in middle cerebral artery territory (Fig. 1). Five patients experienced pontine brainstem infarcts. One patient with right-hand weakness due to left-hemispheric stroke also featured punctuate embolic lesions in both cerebellar hemispheres. However, it is very unlikely that these cerebellar lesions had a relevant impact on hand motor weakness or cortico-cortical connectivity.

Static and dynamic functional network connectivity

After computing time courses and spatial maps of 14 motor components (Fig. 2), we first estimated static connectivity (Fig. 3A). Subsequently, we obtained dFNC via the sliding window approach. Hereupon, we identified three discrete, re-occurring connectivity states via k-means clustering, since the cluster validity index suggested three as an optimal cluster number solution (Fig. 3B).

Group differences in dynamic connectivity variability

The variability in dynamic connectivity of eight network pairs differed significantly between the three patient subgroups with different amounts of initial motor impairment (one-way ANOVA: $P < 0.05$, Fig. 4A, left plot). These differences particularly pertained to connections between the cortical sensorimotor networks and the putamen. Mildly affected patients presented with generally lower variability values than both moderately-to-severely and non-affected patients (*post hoc* *t*-tests: $P < 0.05$, FDR-corrected, Fig. 4B,

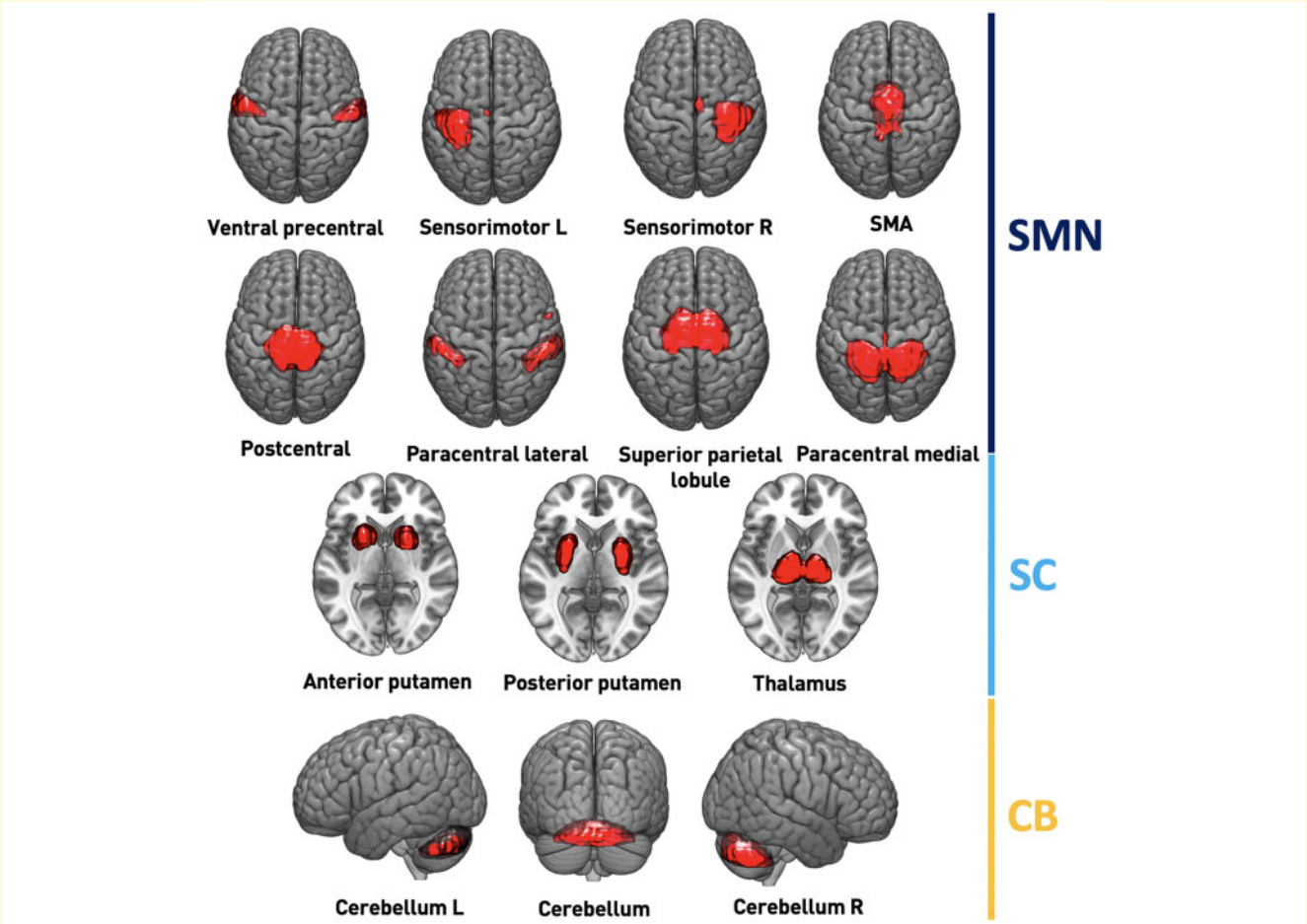

Figure 2 Spatial maps of 14 included intrinsic connectivity networks. Networks were organized in three motor-related functional domains: Sensorimotor (SMN, 8 components, *dark blue*), subcortical (SC, 3 components, *light blue*) and cerebellar (CB, 3 components, *yellow*). Back-reconstruction of networks was based on components extracted in Allen et al.[9] L, left; R, right; SMA, supplementary motor area.

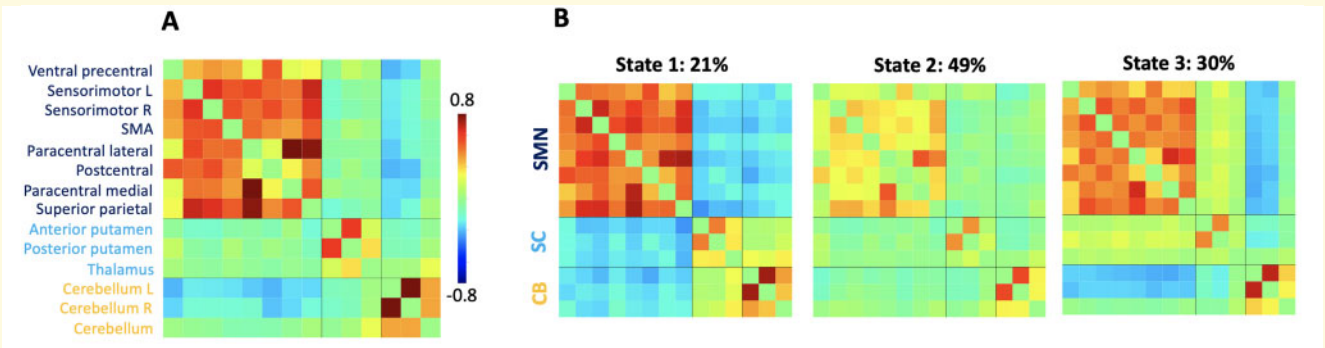

Figure 3 (A) Static and (B) Dynamic functional network connectivity. (**A**) Darker red colour implies stronger positive, darker blue stronger negative connectivity. Static functional connectivity was, therefore, characterized by strong positive intra-domain connectivity, neutral connectivity between cortical and subcortical motor networks as well as neutral to negative connectivity between either cortical and subcortical motor networks and cerebellar networks. (**B**) Stated percentages above each state correspond to state-specific fraction times across all subjects. State 1, the most seldom state (median dwell time: 10 windows), featured highly positive intra-domain connectivity and highly negative connectivity between the sensorimotor and subcortical as well as cerebellar domains. In contrast, State 2, which emerged most often (median dwell time: 22 windows), was characterized by particularly weak intra-domain connectivity and mostly neutral inter-domain connectivity. Lastly, State 3 presented highly positive intra-domain connectivity, neutral connectivity between the sensorimotor and subcortical, and slightly negative connectivity between sensorimotor and cerebellar domains (median dwell time: 14 windows). We can also notice that visually static functional connectivity resembled State 3 the most. This observation is supported by obtaining the smallest l_1-distance from the static functional connectivity state to all three connectivity states.

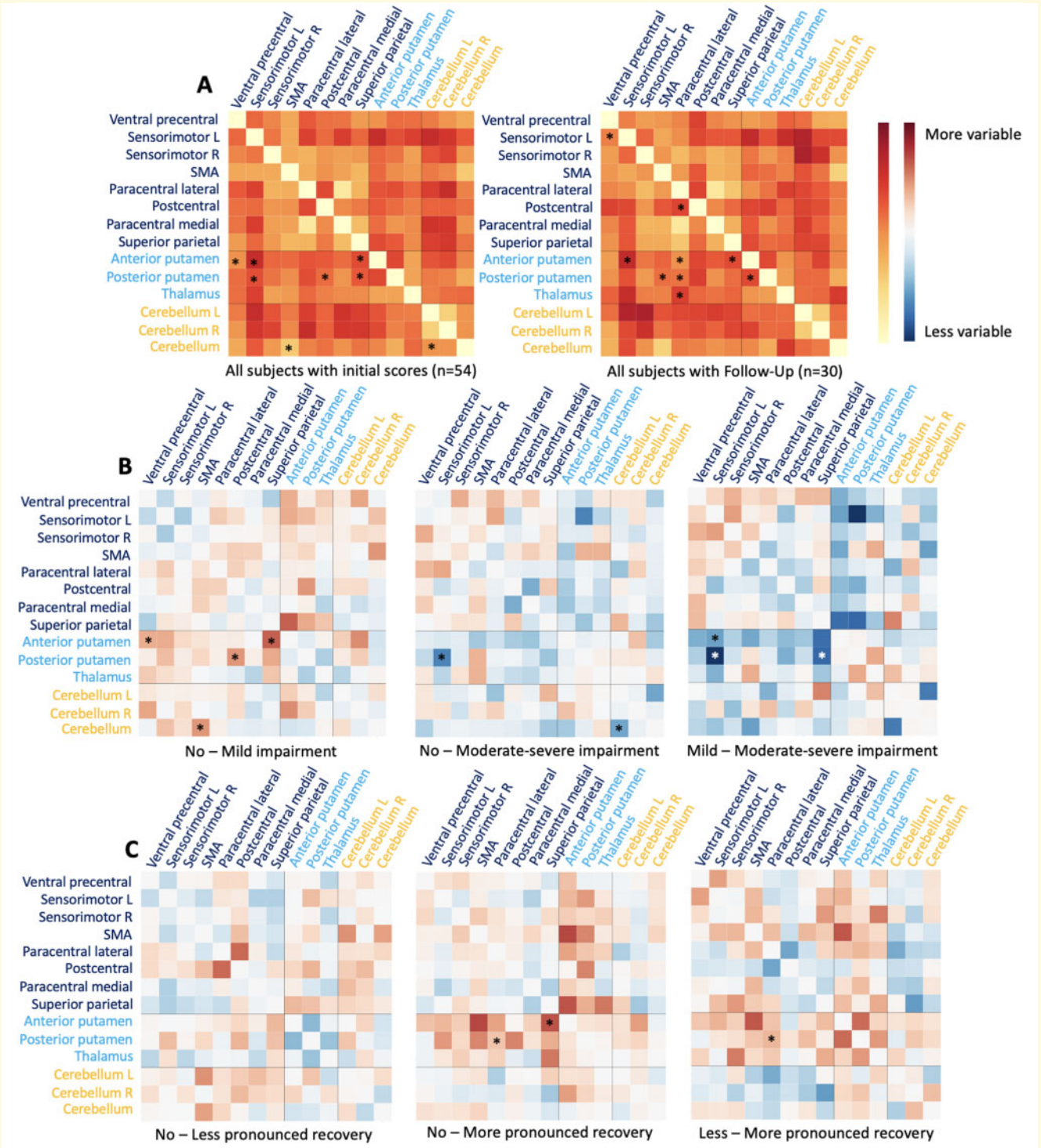

Figure 4 Dynamic functional connectivity strength variability in relation to upper limb motor impairments and recovery post-stroke. (**A**) Mean variability of dynamic connectivity throughout the entire scan session. The left plot visualizes the variability averaged over all 54 patients initially recruited. The right plot considers all 30 patients that were followed up after six months. Darker red colour represents higher variability values. Asterisks indicate significant group effects between patients with no, moderate, or severe upper limb impairments or more, less or no recovery, respectively (three-level one-way ANOVA: $P < 0.05$). Most of the differences in variability were found for connections between the bilateral putamen and cortical sensorimotor networks. (**B**) Subtraction maps of mean variability values between each subgroup constellation of initial impairment. Red colour implies higher variability values, blue colour lower variability values. *Post hoc* *t*-tests revealed some overlapping ('posterior putamen–left sensorimotor cortex'), yet mostly distinct significantly different connectivity pairs between mildly affected patients and non-affected patients, as well as mildly and moderately-to-severely affected patient groups ($P < 0.05$, FDR-corrected for multiple comparisons). Mildly affected patients differed from non-affected patients in more dynamic connectivity variability pairs than did moderately-to-severely affected patients (four versus two pairs). (**C**) Subtraction maps of mean variability values between each subgroup constellation of recoverees. The asterisk on the right indicates a significant group effect between patients with more pronounced versus those with less pronounced motor recovery post-stroke (*t*-test: $P < 0.05$, FDR-corrected for multiple comparisons).

Table 2 Prediction of acute motor impairment (out-of-sample AUC and 95% confidence interval)

	No. of subjects	5-component structural data	28-component structural data	Static connectivity data	Dynamic transitions, fraction and dwell times data	Dynamic variability data
Acute MI-UL: No-motor impairment versus motor impairment	**Structural:** 53 (27 versus 26, 49% without motor symptoms) **fMRI:** 54 (28 versus 26, 48% without motor symptoms)	0.61 ± 0.02	0.59 ± 0.01	0.62 ± 0.02	**0.67 ± 0.01***	0.34 ± 0.01
Acute MI-UL: Mild motor impairment versus moderate-severe motor impairment	**Structural:** 27 (16 versus 11, 59% with mild motor impairments) **fMRI:** 28 (16 versus 12, 57% with mild motor impairments)	0.22 ± 0.02	0.33 ± 0.02	0.32 ± 0.01	0.34 ± 0.02	**0.83 ± 0.02***

The highest prediction performances per scenario are stated in bold and marked with an asterisk.

outer plots). Moderately-to-severely affected patients presented with even higher dynamic connectivity variability than non-affected patients (*post hoc t*-tests: $P < 0.05$, FDR-corrected, Fig. 4B, middle plot).

When contrasting the three patient subgroups with different amounts of motor recovery over time, we substantiated nine significantly different dynamic connectivity variability pairs, (one-way ANOVA: $P < 0.05$, Fig. 4A, right plot). Patients in the substantial recovery subgroup were particularly characterized by a lower variability in dynamic connectivity between the supplementary motor area (SMA) and bilateral posterior putamen (*post hoc t*-tests: $P < 0.05$, FDR-corrected, Fig. 4C, middle and right plots). The overall variability in dFNC strength weakly correlated with lesion volume ($r = 0.29$, $P = 0.04$). There was, however, no correlation between the overall variability and change in motor performance ($r = -0.06$, $P = 0.82$).

Prediction of acute upper limb impairment

When aiming to predict acute upper limb impairment in the entire sample of 54 stroke subjects, the highest prediction performance was achieved by the dynamic fraction and dwell times data [out-of-sample AUC ± 95% confidence interval (CI): 0.67 ± 0.01]. Feature importances indicated that the total time spent in state 3, i.e. the fraction time in a functionally markedly integrated state, was the most relevant parameter for predicting the acute impairment status (c.f., Supplemental materials for a quantitative evaluation of integration and segregation). Dwell times in state 2, another functionally integrated state, were assigned the second highest feature importance. Both features, however, did not correlate with acute motor impairments (fraction time state 3: $\rho = 0.22$, $P = 0.12$; dwell time state 2: $\rho = 0.03$, $P = 0.87$), which may be indicative of more complex interaction and non-linear effects that the random forest classifier picked up on. The models based on the structural, as well as static functional connectivity data performed second-best (5-component structural: AUC = 0.61 ± 0.02, 28-component structural: AUC = 0.59 ± 0.01, static connectivity: AUC = 0.62 ± 0.02). The model considering the dynamic variability data performed significantly worse than the previous models and achieved an AUC at chance level (Table 2, Supplementary Table 2).

However, when refining the prediction scenario to the distinction between patients with moderate-to-severe and mild motor impairments ($n = 28$), it was the model based on dynamic connectivity variabilities that demonstrated the highest prediction capacity (AUC = 0.83 ± 0.02). The amount of motor impairment was especially predicted by the variability of dynamic connectivity between the ipsilesional sensorimotor network and bilateral posterior putamen, as well as ventral pre-central cortex and bilateral anterior putamen (Fig. 5). Here, more severe motor impairments correlated with higher variability in these networks (ipsilesional sensorimotor network–posterior putamen: $\rho = -0.57$, $P = 0.001$, ventral pre-central cortex–anterior putamen: $\rho = -0.40$, $P = 0.035$). None of the other models provided a prediction fidelity above the level of chance for the distinction between impairment levels (Table 2).

In summary, the presence of acute motor impairments was best predicted by the fraction and dwell times-based dynamic connectivity model. In contrast, the variability of individual dynamic connectivity pairs was a powerful predictor of the amount of motor impairment.

Prediction of motor recovery

We next challenged the capacity of acutely acquired structural and rsfMRI data to predict motor recovery 6 months after stroke ($n = 30$). The motricity index score obtained in the acute post-stroke phase was already a strong predictor, when differentiating between more and less pronounced, as well as no changes in motor function in the first six months post-stroke (AUC = 0.84 ± 0.01, all results: Table 3, Supplementary Table 3). The joint model based on the dynamic fraction and dwell times data and the acute motricity index score accomplished a prediction performance of AUC = 0.89 ± 0.01. The 95% confidence intervals of this joint model did not overlap

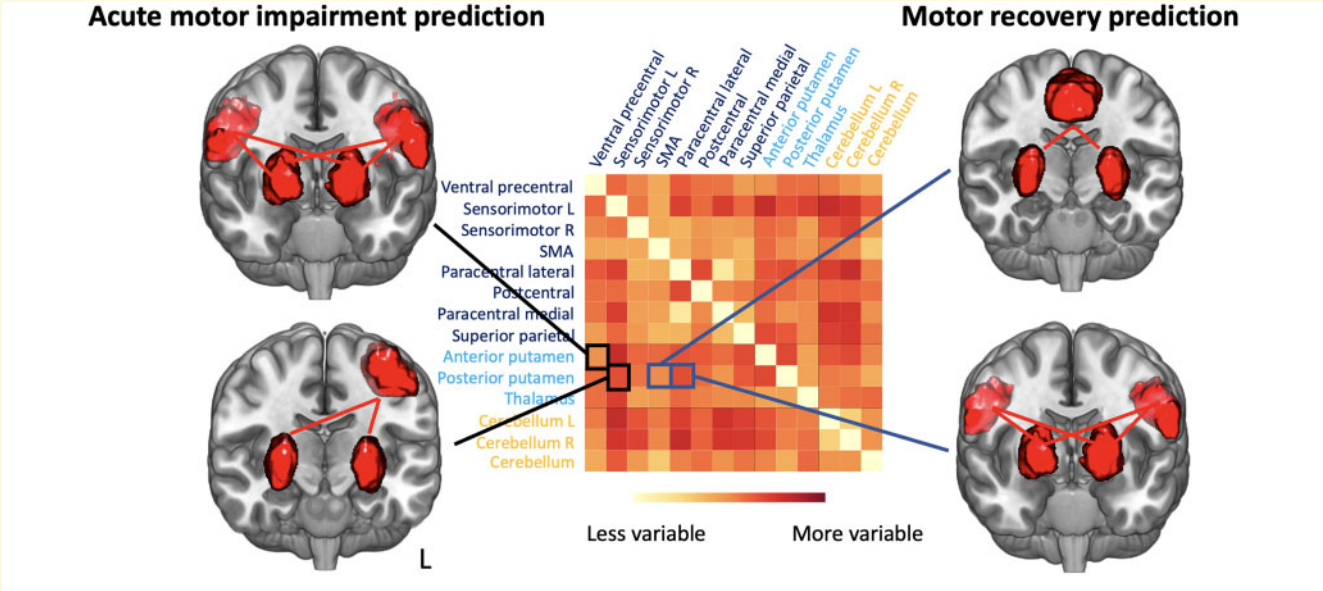

Figure 5 Variability of dynamic connectivity and feature importances. Brain renderings visualize the most predictive dynamic connectivity variability pairs for the prediction of mild versus moderate-severe acute motor impairments (*left*) and the prediction of more or less pronounced recovery in the patients with initial impairment in the first months after stroke (*right*). The variabilities in dynamic connectivity between SMA and bilateral posterior putamen, as well as lateral paracentral cortex and bilateral posterior putamen were the most relevant for predicting recovery. Correlation analyses revealed that patients with more pronounced recovery featured less variability in these connections.

with the 95% confidence interval of the model using the MI as the sole predictor variable, highlighting significantly improved prediction performance when adding the dynamic connectivity parameters to the behavioural data. The two most important features were the number of transitions between states and fraction time in state 3, i.e. a functionally integrated state. The acute MI-UL score was ranked as the third most important feature only. Both of the most important dynamic connectivity parameters correlated negatively with the recovery, i.e. the more a subject recovered, the shorter their time spent in state 3 was and the fewer they switched between different states (Fraction time state 3: $\rho = -0.49$, $P = 0.006$; Number of state transitions: $\rho = -0.39$, $P = 0.04$).

Finally, we tested the prediction performance when only considering patients with an initial impairment. In this scenario, the amount of recovery (no-minor versus substantial) was best predicted by the dynamic fraction and dwell times data (AUC $= 0.92 \pm 0.02$, Table 3, Supplementary Tables 4 and 5). The most important features were fraction and dwell times in state 3, i.e. a functionally integrated state (Fraction time state 3: $\rho = -0.56$, $P = 0.02$; Dwell time state 3: $\rho = -0.61$, $P = 0.008$). The model relying on the initial MI-score achieved a significantly lower AUC of 0.82 (AUC $= 0.82 \pm 0.02$). It was paralleled in performance by the models considering the variability in dynamic connectivity (with the addition of the MI-score: AUC $= 0.83 \pm 0.02$ and without the MI-score: AUC $= 0.82 \pm 0.02$). The two top ranked features were the variability in dynamic connectivity between SMA and bilateral posterior putamen, as well as lateral paracentral cortex and bilateral posterior putamen. Correlation analyses indicated that subjects showed higher recovery values the smaller variability was in these connections (SMA–putamen: $\rho = -0.59$, $P = 0.01$; lateral paracentral cortex–lateral paracentral cortex: $\rho = -0.54$, $P = 0.03$). While the models relying on 28-component structural and static connectivity data did not exceed a chance-level prediction performance, the model incorporating 5-component structural data had (i) an AUC of 0.72 ± 0.03 with the addition of the MI-score, and (ii) 0.66 ± 0.02 without the MI-score. This finding indicates some relevance of the stroke lesion location with respect to the potential to recover.

In conclusion, we found dFNC parameters obtained in the first days post-stroke such as the state-specific fraction and dwell times as well as the variability of dynamic connectivity to be potent predictors of motor recovery six months later. In particular, fraction and dwell times significantly enhanced prediction performance beyond the level of traditional and well-known clinical predictors, such as the initial motor impairment.

Discussion

We here explored novel predictors of individual acute motor impairment and recovery after stroke. These biomarkers were derived from dFNC analyses of rsfMRI

Table 3 Prediction of upper limb motor recovery based on structural MRI data, static and dynamic connectivity (out-of-sample AUC and 95% confidence interval)

	No. of subjects	Acute MI-UL	5-component structural data & acute MI-UL	28-component structural data & acute MI-UL	Static connectivity data and acute MI-UL	Dynamic transitions, fraction and dwell times data & acute MI-UL	Dynamic variability data & acute MI-UL
MI-UL Recovery: Three-group classification	**Structural and fMRI:** 30 (16 versus 5 versus 9, with no, less and more pronounced motor recovery)	0.84 ± 0.01	0.75 ± 0.02	0.72 ± 0.02	0.67 ± 0.02	**0.89 ± 0.01***	**0.74 ± 0.01**
MI-UL Recovery: More and less pronounced recovery	**Structural and fMRI:** 17 (9 versus 8, 53% with more pronounced motor recovery)	0.82 ± 0.02	0.72 ± 0.03	0.52 ± 0.03	0.25 ± 0.01	**0.92 ± 0.02***	0.83 ± 0.02

The highest prediction performances per scenario are stated in bold and marked with an asterisk.

data from 54/30 acute ischaemic stroke patients that presented with varying degrees of motor impairment. DFNC analyses are special because they allow for the extraction of moment-to-moment fluctuations in brain connectivity and the definition of re-occurring dynamic connectivity states.[9,10] Thereby, this approach increases the time resolution of resting-state fMRI evaluations to seconds and may be particularly capable of capturing stroke-induced short-lasting connectivity alterations and higher network flexibility.[12,14,34] Fraction times in state 3, i.e. the total time spent in a functionally integrated connectivity state, and the variability in dynamic connectivity between putamen and various cortical sensorimotor areas crystallized as particularly promising biomarkers for individualized outcome predictions.

Functional segregation and integration

Stroke patients with or without acute motor impairments were most accurately differentiated based on the time spent in specific connectivity states. Feature importance highlighted fraction times in state 3, a connectivity state that was characterized by pronounced functional integration. *Functional integration* here describes a synchronized information processing between various functional domains, while *functional segregation* implies more isolated information processing within functional domains.[35] Previous studies of dynamic connectivity in two independent acute ischaemic stroke cohorts have already uncovered links between functional integration and segregation and motor performance: lower motor domain integration in case of severe compared to moderate hand motor impairments[12] and increased whole-brain segregation (i.e. decreased integration) in case of a high stroke severity.[36] Importantly, data of these two cohorts were completely non-overlapping with the present one, in particular, they were obtained in scanners with different field strengths (3 T instead of 1.5 T), at different time points or places. Interestingly, in healthy subjects with cast-induced motor inactivity of the upper limb, motor network topology also turned into a more segregated state.[37] We here did not observe a clear correlation between fraction times in integrated state 3 and acute motor impairment across all subjects. Rather, our random forest classifier approach may have enabled us to differentiate between groups by also capturing non-linear, as well as interaction effects between more than one variable.

While we did not find an association between fraction times in state 3 and acute motor impairments, we did, however, identify a high capacity of the fraction and dwell times in state 3 to predict and correlate with future recovery. Patients that did not show a preference for this spatially integrated connectivity state in the first days after stroke recovered more substantially in the upcoming weeks. From a pathomechanistic perspective, the possibly most striking characteristic of state 3 is the pattern of highly positive intra-domain dynamic connectivity in combination with a positive connectivity between cortical and subcortical networks. Hence, the association of lower fraction and dwell times in state 3 with motor recovery indicates that a more segregated, isolated processing within the cortical and subcortical motor domains may be mechanistically critical for a more successful stroke recovery. Interestingly, increased segregation, i.e. decreased integration, has been previously linked to expedited regain of cognitive function in healthy ageing and diffusely damaged brains after mild traumatic brain injury.[38] Our current findings are, therefore, in line with these reports.

Variability of dynamic connectivity

By considering the variability in dynamic connectivity, we here amend the previously employed toolset to generate insights into the role of motor areas in healthy and pathological motor function. In inference- and prediction-

focussed analyses, we were able to link mild motor impairment as well as a more pronounced recovery to lower, i.e. more stable, dynamic connectivity variability values in select cortical–subcortical connections. The investigation of dynamic connectivity variability profiles was previously motivated by Allen et al.,[9] especially as they represented inaccessible information content when conducting static connectivity analyses. The authors described distinct 'zones of instability', i.e. regions with more variable dynamic connectivity in healthy volunteers: The most variable regions were located in the lateral parietal and occipital cortex. Comparable analyses of dFNC variability in neurological patients with temporal lobe epilepsy inferred the instability of precuneus dynamic connectivity as a signature of the disease.[39] In yet another study, the dFNC variability provided powerful information for the differentiation between Alzheimer's patients and healthy controls.[15]

In this study, it was the variability of the dynamic connectivity between the ipsilesional sensorimotor cortex and bilateral posterior putamen that predicted a more versus less initial impairment especially well. Statistical group comparisons moreover suggested that, both moderately-to-severely affected patients, as well as those without any impairments had a higher ipsilesional sensorimotor-putamen dFNC variability than mildly affected patients. Both of these brain regions are well known to be implicated in the emergence of acute motor impairments and recovery post-stroke. Lesion symptom mapping studies repeatedly reported ischaemic lesions in the putamen underlying upper limb impairment.[40] Furthermore, the link between lower (static) resting-state connectivity between ipsi- and contralesional motor areas and higher motor impairment is one of the most prominently featured findings in stroke neuroimaging research.[8,41] The connectivity between the posterior ipsilesional sensorimotor cortex and putamen, let alone their dFNC variability, however, requires further exploration to determine the biological meaning.

In case of predicting motor recovery, the variability of the dynamic connectivity strengths between the SMAs and the bilateral posterior parts of the putamen was the most predictive feature. This SMA–putamen variability was also found to be significantly lower in case of more pronounced recovery compared to less pronounced and no change in motor function. The SMA has been consistently identified as critical region for physiological motor function as well as for stroke recovery in previous studies.[42,43] In particular, longitudinal motor-task-based functional imaging studies demonstrated a recovery-related excess in activation in these regions early after stroke[42] and decreases in activation in sub-acute and chronic stages after stroke.[43] In addition, dynamic causal modelling analyses that extracted links between increases in SMA-M1 coupling and motor improvements suggested a supportive role of SMA for motor recovery post-stroke.[44] Lastly, diffusion-tensor imaging in healthy adults indicates structural connections between SMA and especially posterior parts of the putamen, highlighting the role of this connection for motor function.[45] In line with this conclusion, the SMA–putamen connectivity was found to be disturbed in patients suffering from motor impairments due to Parkinson's disease.[46,47]

In summary, previous results on dFNC variability and ours combined suggest that these dFNC parameters represent biologically meaningful fingerprints of neurological diseases. In the case of ischaemic stroke, this variability might particularly well capture the effects of brain injury and early plasticity mechanism in the first few days post-stroke.

Limitation and future directions

A sample of 54 stroke subjects is still extendible if intended for the construction of outcome prediction models, especially as the sample size was decreased further in ancillary analyses. We obtained out-of-sample estimates of model performance via 5-fold cross-validation in all cases, as is the current recommendation in neuroimaging-based prediction studies.[48] However, future studies, relying on external, i.e. independent datasets, are warranted to test the generalizability of our findings in further depths and ensure that predictions generated from the here developed models continue to be accurate in new patient samples. These steps may then facilitate a smoother translation into the clinical routine. Of note, the present dataset is among the largest acute stroke rsfMRI datasets currently available and rendered particularly unique by its comprehensive longitudinal motor assessment and acquisition during the clinical routine, i.e. when the patients received their diagnostic MR scans. The latter circumstance enabled a very early time point of data acquisition, on average 2.5 days after stroke. This very early time point of data acquisition contrasts other larger-scale stroke imaging studies, that have recruited subjects on average two weeks after index stroke.[7] Altogether, our study underlines the general feasibility of implementing the approach presented here with respect to clinical translation. Owing to the task-free nature of rsfMRI, it was also feasible to recruit stroke patients that are typically excluded from fMRI task studies, i.e. patients with severe motor impairment. Despite the task-free nature, it nonetheless remains essential to minimize any artefacts due to motion in the scanner, which might be particularly challenging in severely affected and also older patients.

Another limitation of this study relates to the fact that we did not systematically assess the amount of rehabilitation therapy that each patient received. However, we can assume that therapy doses varied between patients given their differences in initial deficits and ensuing recovery, since the amount of rehabilitation therapy in Germany is usually decided based on the progress a patient makes. Altogether, it is therefore very difficult, if not impossible, to anticipate the exact amount of rehabilitation, that a

patient will receive later. Hence, such information cannot be reliably included into prediction algorithms at the beginning of the recovery process.[49] Along these lines, we here predicted the amount of recovery based on factors, such as symptom severity and connectivity estimates, *before* rehabilitation was commenced. It thus appears likely that differences in the absolute amount of recovery were not primarily driven by differences in rehabilitation minutes.

Our findings suggest that the variability of several dynamic connectivity pairs is relevant for motor impairment as well as for recovery. We were also able to extract a weak positive correlation between the overall variability of dynamic connectivity and lesion volume. It was, however, beyond the scope of the current study to determine detailed links between this variability and individual lesion locations given their large spatial variability (c.f., Fig. 1). Such associations could, for example, be investigated further in larger samples via canonical correlation analyses[50] that aim to find joint associations between sets of variables from different modalities.

Lastly, we have focused on classification scenarios, i.e. our prediction models discriminated patients with or without motor impairments. It could thus be a valuable next step to predict outcomes on continuous scales, i.e. predict the precise amount of impairment per patient. Moreover, it will be important to extend the validity of our findings based on the Motricity Index, a very quick and well validated instrument to capture motor impairments,[51,52] to further frequently used impairment and activity limitation scales, such as the Fugl-Meyer Assessment of the upper extremity (FU-UE)[53] or the Action Research Arm Test (ARAT).[54] In particular, these more detailed tests may offer the possibility of specifically evaluating subgroups of patients with respect to already established minimal clinically important differences (MCID),[55] that may identify motor recovery that has a noticeable and meaningful impact on patients' lives.[49,56] Lastly, future studies may further elucidate the interplay between behavioural and imaging-based biomarkers of stroke recovery. In the present study, the model incorporating dynamic connectivity information provided the significantly highest prediction performance. However, it has to be noted that the initial behavioural motor score itself was already an effective predictor of stroke recovery. While we may generally be interested in the highest possible prediction performance—as it can, indeed, make a difference on the level of the individual patient—this small difference in prediction performance may justify a focus on easy-to-obtain behavioural measures for prediction in case of limited resources.

Conclusions

Our data show that dynamic connectivity measures contain a high predictive capacity not only for acute impairments but also for the potential of recovery following stroke. Especially dynamic connectivity estimates between the putamen and cortical motor networks emerged as reliable predictors of motor impairment and recovery. In conclusion, our study highlights the value of dynamic connectivity-derived information to gain insights into the phenotypes of acute ischaemic brain injury and recovery after stroke.

Supplementary material

Supplementary material is available at *Brain Communications* online.

Acknowledgements

We are grateful to our colleagues at the Department of Neurology, University Hospital Cologne & Medical Faculty, University of Cologne, for valuable support and discussions. Furthermore, we are grateful to our research participants without whom this work would not have been possible.

Funding

A.K.B. is supported by a travel stipend from the German Section of the International Federation of Clinical Neurophysiology [Deutsche Gesellschaft für Klinische Neurophysiologie und funktionelle Bildgebung (DGKN)]. V.D.C. is supported in part by National Institutes of Health (NIH) grant R01DA040487. N.S.R. is in part supported by National Institutes of Health(NIH) and National Institute of Neurological Disorders and Stroke (NINDS) (R01NS082285, R01NS086905, U19NS115388). G.R.F. gratefully acknowledges support by the Magda- and Walter Boll foundation. G.R.F. and C.G. are funded by the Deutsche Forschungsgemeinschaft (DFG, German Research Foundation)—Project-ID 431549029—SFB 1451, project C05.

Competing interests

N.S.R. has received compensation as scientific advisory consultant from Omniox, Sanofi Genzyme and AbbVie Inc.

References

1. Benjamin EJ, Blaha MJ, Chiuve SE, et al. American Heart Association Statistics Committee and Stroke Statistics Subcommittee. Heart disease and stroke statistics-2017 update: A report from the American Heart Association. *Circulation*. 2017; 135(10):e146–e603.
2. Hay SI, Abajobir AA, Abate KH, et al. Global, regional, and national disability-adjusted life-years (DALYs) for 333 diseases and injuries and healthy life expectancy (HALE) for 195 countries and territories, 1990–2016: A systematic analysis for the Global Burden of Disease Study 2016. *Lancet*. 2017;390(10100):1260–1344.

3. Prabhakaran S, Zarahn E, Riley C, et al. Inter-individual variability in the capacity for motor recovery after ischemic stroke. *Neurorehabil Neural Repair*. 2008;22(1):64–71.
4. Kundert R, Goldsmith J, Veerbeek JM, Krakauer JW, Luft AR. What the proportional recovery rule is (and is not): Methodological and statistical considerations. *Neurorehabil Neural Repair*. 2019; 33(11):876–887.
5. Bonkhoff AK, Hope T, Bzdok D, et al. Bringing proportional recovery into proportion: Bayesian modelling of post-stroke motor impairment. *Brain*. 2020;143(7):2189–2206.
6. Rehme AK, Volz LJ, Feis D-L, Eickhoff SB, Fink GR, Grefkes C. Individual prediction of chronic motor outcome in the acute post-stroke stage: Behavioral parameters versus functional imaging. *Hum Brain Mapp*. 2015;36(11):4553–4565.
7. Siegel JS, Ramsey LE, Snyder AZ, et al. Disruptions of network connectivity predict impairment in multiple behavioral domains after stroke. *Proc Natl Acad Sci USA*. 2016;113(30): E4367–E4376.
8. Rehme AK, Volz LJ, Feis D-L, et al. Identifying neuroimaging markers of motor disability in acute stroke by machine learning techniques. *Cereb Cortex*. 2015;25(9):3046–3056.
9. Allen EA, Damaraju E, Plis SM, Erhardt EB, Eichele T, Calhoun VD. Tracking whole-brain connectivity dynamics in the resting state. *Cereb Cortex*. 2014;24(3):663–676.
10. Calhoun VD, Miller R, Pearlson G, Adalı T. The chronnectome: Time-varying connectivity networks as the next frontier in fMRI data discovery. *Neuron*. 2014;84(2):262–274.
11. Vidaurre D, Llera A, Smith SM, Woolrich MW. Behavioural relevance of spontaneous, transient brain network interactions in fMRI. *Neuroimage*. 2021;229:117713.
12. Bonkhoff AK, Espinoza FA, Gazula H, et al. Acute ischaemic stroke alters the brain's preference for distinct dynamic connectivity states. *Brain*. 2020;143(5):1525–1540.
13. Rashid B, Arbabshirani MR, Damaraju E, et al. Classification of schizophrenia and bipolar patients using static and dynamic resting-state fMRI brain connectivity. *Neuroimage*. 2016;134:645–657.
14. Vergara VM, Mayer AR, Kiehl KA, Calhoun VD. Dynamic functional network connectivity discriminates mild traumatic brain injury through machine learning. *Neuroimage Clin*. 2018;19:30–37.
15. de Vos F, Koini M, Schouten TM, et al. A comprehensive analysis of resting state fMRI measures to classify individual patients with Alzheimer's disease. *Neuroimage*. 2018;167:62–72.
16. Demeurisse G, Demol O, Robaye E. Motor evaluation in vascular hemiplegia. *Eur Neurol*. 1980;19(6):382–389.
17. Volz LJ, Rehme AK, Michely J, et al. Shaping early reorganization of neural networks promotes motor function after stroke. *Cereb Cortex*. 2016;26(6):2882–2894.
18. Rorden C, Brett M. Stereotaxic display of brain lesions. *Behav Neurol*. 2000;12(4):191–200.
19. Ashburner J, Friston KJ. Unified segmentation. *Neuroimage*. 2005; 26(3):839–851.
20. Lin Q-H, Liu J, Zheng Y-R, Liang H, Calhoun VD. Semiblind spatial ICA of fMRI using spatial constraints. *Hum Brain Mapp*. 2010;31(7):1076–1088.
21. Du Y, Fan Y. Group information guided ICA for fMRI data analysis. *Neuroimage*. 2013;69:157–197.
22. Salman MS, Du Y, Lin D, et al. Group ICA for identifying biomarkers in schizophrenia: 'Adaptive' networks via spatially constrained ICA show more sensitivity to group differences than spatio-temporal regression. *Neuroimage Clin*. 2019;22:101747.
23. Rachakonda S, Egolf E, Correa N, Calhoun V. Group ICA of fMRI toolbox (GIFT) manual. *Dostupné z* http://www nitrc org/docman/view php/55/295/v1 3d_ GIFTManual pdf (5 November 2011, date last accessed); 2007.
24. Damaraju E, Allen EA, Belger A, et al. Dynamic functional connectivity analysis reveals transient states of dysconnectivity in schizophrenia. *Neuroimage Clin*. 2014;5:298–308.
25. Sakoğlu Ü, Pearlson GD, Kiehl KA, Wang YM, Michael AM, Calhoun VD. A method for evaluating dynamic functional network connectivity and task-modulation: Application to schizophrenia. *Magn Reson Mater Phys Biol Med*. 2010;23(5-6):351–366.
26. Preti MG, Bolton TA, Van De Ville D. The dynamic functional connectome: State-of-the-art and perspectives. *Neuroimage*. 2017; 160:41–54.
27. Friedman J, Hastie T, Tibshirani R. Sparse inverse covariance estimation with the graphical lasso. *Biostatistics*. 2008;9(3):432–441.
28. Lloyd S. Least squares quantization in PCM. *IEEE Trans Inf Theory*. 1982;28(2):129–137.
29. Aggarwal CC, Hinneburg A, Keim DA. On the surprising behavior of distance metrics in high dimensional space. In: *International Conference on Database Theory*. Berlin, Heidelberg: Springer; 2001:420–434.
30. Espinoza FA, Turner JA, Vergara VM, et al. Whole-brain connectivity in a large study of Huntington's disease gene mutation carriers and healthy controls. *Brain Connect*. 2018;8(3):166–178.
31. Breiman L. Random forests. *Mach Learn*. 2001;45(1):5–32.
32. James G, Witten D, Hastie T, Tibshirani R. *An Introduction to Statistical Learning*, Vol. 112. New York: Springer; 2013.
33. Olson RS, Cava WL, Mustahsan Z, Varik A, Moore JH. Data-driven advice for applying machine learning to bioinformatics problems. *Pac Symp Biocomput*. 2018;23:192–203.
34. Horn HJ, van der Vergara VM, Espinoza FA, et al. Functional outcome is tied to dynamic brain states after mild to moderate traumatic brain injury. *Hum Brain Mapp*. 2020;41(3):617–631.
35. Friston KJ. Functional and effective connectivity: A review. *Brain Connect*. 2011;1(1):13–36.
36. Bonkhoff AK, Schirmer MD, Bretzner M, et al. Abnormal dynamic functional connectivity is linked to recovery after acute ischemic stroke. *Hum Brain Mapp*. 2021;42(7):2278–2291.
37. Newbold DJ, Laumann TO, Hoyt CR, et al. Plasticity and spontaneous activity pulses in disused human brain circuits. *Neuron*. 2020;107(3):580–589.e6.
38. Gallen CL, D'Esposito M. Brain modularity: A biomarker of intervention-related plasticity. *Trends Cogn Sci*. 2019;23(4):293–304.
39. Robinson LF, He X, Barnett P, et al. The temporal instability of resting state network connectivity in intractable epilepsy. *Hum Brain Mapp*. 2017;38(1):528–540.
40. Findlater SE, Hawe RL, Mazerolle EL, et al. Comparing CST lesion metrics as biomarkers for recovery of motor and proprioceptive impairments after stroke. *Neurorehabil Neural Repair*. 2019; 33(10):848–861.
41. Carter AR, Astafiev SV, Lang CE, et al. Resting interhemispheric functional magnetic resonance imaging connectivity predicts performance after stroke. *Ann Neurol*. 2010;67(3):365–375.
42. Rehme AK, Fink GR, von Cramon DY, Grefkes C. The role of the contralesional motor cortex for motor recovery in the early days after stroke assessed with longitudinal FMRI. *Cereb Cortex*. 2011; 21(4):756–768.
43. Ward NS, Brown MM, Thompson AJ, Frackowiak RSJ. Neural correlates of motor recovery after stroke: A longitudinal fMRI study. *Brain*. 2003;126(Pt 11):2476–2496.
44. Rehme AK, Eickhoff SB, Wang LE, Fink GR, Grefkes C. Dynamic causal modeling of cortical activity from the acute to the chronic stage after stroke. *Neuroimage*. 2011;55(3):1147–1158.
45. Lehéricy S, Ducros M, Van de Moortele P-F, et al. Diffusion tensor fiber tracking shows distinct corticostriatal circuits in humans. *Ann Neurol*. 2004;55(4):522–529.
46. Wu T, Wang L, Hallett M, Chen Y, Li K, Chan P. Effective connectivity of brain networks during self-initiated movement in Parkinson's disease. *Neuroimage*. 2011;55(1):204–215.
47. Yu R, Liu B, Wang L, Chen J, Liu X. Enhanced functional connectivity between putamen and supplementary motor area in Parkinson's disease patients. *PLoS One*. 2013;8(3):e59717.
48. Varoquaux G, Raamana PR, Engemann DA, Hoyos-Idrobo A, Schwartz Y, Thirion B. Assessing and tuning brain decoders: Cross-

validation, caveats, and guidelines. *Neuroimage*. 2017;145(Pt B): 166–179.
49. Stinear CM, Smith M-C, Byblow WD. Prediction tools for stroke rehabilitation. *Stroke*. 2019;50(11):3314–3322.
50. Hotelling H. Relations between two sets of variates. In: *Breakthroughs in statistics*. New York, NY: Springer; 1992: 162–190.
51. Collin C, Wade D. Assessing motor impairment after stroke: A pilot reliability study. *J Neurol Neurosurg Psychiatry*. 1990;53(7): 576–579.
52. W Bohannon R. Motricity index scores are valid indicators of paretic upper extremity strength following stroke. *J Phys Ther Sci*. 1999;11(2):59–61.
53. Fugl-Meyer AR, Jääskö L, Leyman I, Olsson S, Steglind S. The post-stroke hemiplegic patient. 1. a method for evaluation of physical performance. *Scand J Rehabil Med*. 1975;7(1):13–31.
54. Yozbatiran N, Der-Yeghiaian L, Cramer SC. A standardized approach to performing the action research arm test. *Neurorehabil Neural Repair*. 2008;22(1):78–90.
55. Page SJ, Fulk GD, Boyne P. Clinically important differences for the upper-extremity Fugl-Meyer Scale in people with minimal to moderate impairment due to chronic stroke. *Phys Ther*. 2012;92(6): 791–798.
56. Haley SM, Fragala-Pinkham MA. Interpreting change scores of tests and measures used in physical therapy. *Phys Ther*. 2006; 86(5):735–743.